Modeling actuation of ionomer cilia in salt solution under an external electric field

Alain Boldini Maxwell Rosen Maurizio Porfiri*

Department of
Mechanical and Aeronautical Engineering
New York University
Tandon School of Engineering
Brooklyn, New York 11201

Youngsu Cha

Center for Intelligent & Interactive Robotics Korea Institute of Science and Technology Seoul, 02792 Republic of Korea

A recent experiment by Kim's group from the University of Nevada, Las Vegas has shown the possibility of actuating ionomer cilia in salt solution. When these actuators are placed between two external electrodes, across which a small voltage is applied, they move toward the cathode. This is in stark contrast with ionic polymer metal composites, where the same ionomers are plated by metal electrodes but bending occurs toward the anode. Here, we seek to unravel the factors underlying the motion of ionomer cilia in salt solution through a physically-based model of actuation. In our model, electrochemistry is described through the Poisson-Nernst-Planck system in terms of concentrations of cations and anions and voltage. Through finite element analysis, we establish that Maxwell stress is the main driving force for the motion of the cilia. This study constitutes a first effort toward understanding the motion of ionomer cilia in salt solution, which, in turn, may help elucidate the physical underpinnings of actuation in ionic polymer metal composites.

1 Introduction

The range of applications of ionic polymer metal composites (IPMCs) has been recently expanding due to the advances in freeform fabrication of ionic membranes [1, 2], which allows for tailoring the performance and geometry of IPMCs. This new class of electroactive materials has been considered for applications as actuators, sensors, and energy harvesters [3–5]. In particular, their large compliance, ability to operate underwater, and small driving voltages have fostered their use in underwater robotics, from robotic fish to jelly fish and manta rays [6].

IPMCs are composite materials that comprise a core ionomer layer and two metal electrodes [4, 5]. Anions are fixed to the backbone of the ionomer, while positively charged counterions can freely move. When a voltage is

*Address all correspondence to this author (also in the Department of Biomedical Engineering). Email: mporfiri@nyu.edu

applied across the IPMC electrodes, the counterions redistribute through the thickness. Their motion generates large osmotic pressure and Maxwell stress [7] in boundary layers near the electrodes, where counterions pile-up (anode) or deplete (cathode). These two physical phenomena (osmotic pressure and Maxwell stress) elicit the macroscopic deformations observed in IPMCs.

Inspired by cilia and flagella in cells, Kim's group from the University of Nevada, Las Vegas recently demonstrated the possibility of actuating ionomer fibers without plated electrodes [8]. (Equivalent predictions have been later confirmed by our group [9].) When placed between two external electrodes in a salt solution, these actuators exhibit consistent motion toward the cathode in response to the applied electric field. This configuration allows to overcome difficulties in material processing encountered with IPMCs, namely, electrode patterning and wiring that could complicate manufacturing and control.

Here, we put forward a modeling framework to describe the actuation of these ionomer fibers. Grounded in physicallybased models of electrochemistry, our approach does not require any fictitious constant, but relies only on physical properties of the material. Due to the difference in time scales and the limited extent of the elastic deformation, the electrochemistry and the mechanical bending are decoupled, whereby the former acts as an input for the latter [10]. The electrochemical model is based on the Poisson-Nernst-Planck (PNP) system [11], which has been widely used for describing electrolytes [12] and ionomer membranes [13]. The field variables of the problem are the concentration of cations, the concentration of anions, and the voltage. As a result of charge imbalance, internal stresses due to ion mixing and polarization (osmotic pressure and Maxwell stress) are generated inside the ionomer. This model is implemented, in a twodimensional setting, in the finite element software COMSOL Multiphysics®. From the simulation, we integrate the internal stresses to estimate the internal bending moments, thereby

pointing at a dominant role played by Maxwell stress.

We start by illustrating the experimental setup in [8] and summarize their results. Then, we describe the electrochemical governing equations of the model, focusing on an approximated finite element solution, and we analyze the results of this simulation. Finally, we highlight future research directions.

2 Experimental results from [8]

Ionomer fibers with a diameter in the range $25-45\,\mu\mathrm{m}$ were manufactured through a melt-drawing process from a Nafion precursor. The fibers were then functionalized to allow counterions' exchange. The setup consisted of a tank with a solution of 0.1 M of lithium chloride (LiCl), in which two external graphite electrodes were suspended (Fig. 1). The distance between the two electrodes was 10 mm and their active submerged area was $100\,\mathrm{mm}^2$. The fiber was clamped with a free length of $42\,\mathrm{mm}$ and positioned between the two external electrodes. The tip actuator was slightly under the electrodes, so that a laser displacement sensor could measure the tip displacement. A $5\,\mathrm{V}$ square-wave $\bar{\psi}$ was applied across the external electrodes. Two frequencies of excitation were tested: $0.1\,\mathrm{Hz}$ and $1\,\mathrm{Hz}$.

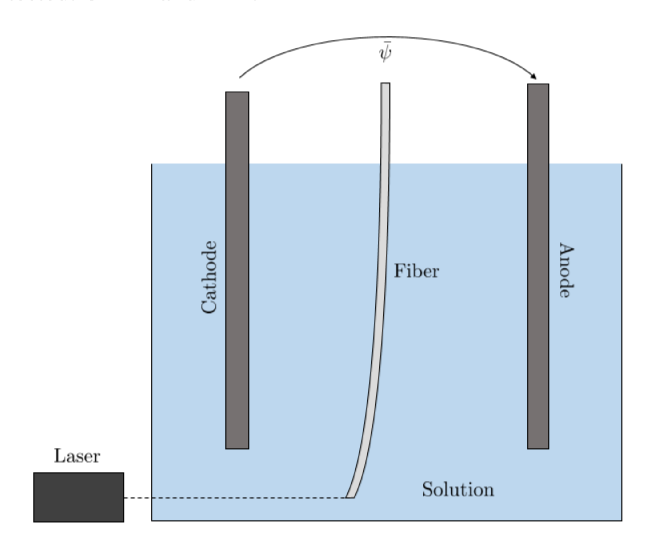


Fig. 1. Schematics of the experimental setup by Kim's group [8]. The ionomer fiber is clamped through an external probe. A laser displacement sensor is used to measure the tip displacement.

The results of the experiments are summarized in Fig. 2. The deflection is always toward the cathode, which is the opposite of what is typically observed in the initial stage of IPMC actuation, before the onset of back-relaxation [5]. A good repeatability of cyclic actuation was registered, suggesting the possibility of using these actuators as biomimetic oscillating cilia. For the $0.1 \, \text{Hz}$ case, the peak-to-peak tip displacement was about 6 mm, while, for the $1 \, \text{Hz}$ case, it was around 1 mm. Likely, this difference was due to water electrolysis. As a control condition, the same experiments were performed in deionized water, with a resistivity of $18.2 \, \text{M}\Omega \, \text{cm}$, indicating a negligible response of the fiber.

3 Modeling framework

Here, we introduce our framework to model the experiment performed in [8]. To simplify the problem, we hypothesize that the deformation has no effect on the electrochemistry. This is motivated by the small displacements observed in [8] and by the separation of the time scales between the electrochemical and mechanical responses [10]. Hence, the electrochemical model is solved for a static domain.

We consider a reference frame with the z-axis aligned with the axis of the actuator, such that the cross-sections lie parallel to the x-y plane, with the x-axis perpendicular to the electrodes. We neglect three-dimensional effects along the vertical (z) direction, and we focus on a two-dimensional problem on an horizontal cross-section (Fig. 3).

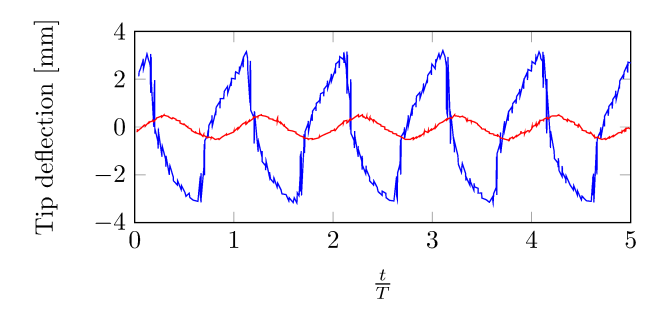


Fig. 2. Time trace of the tip displacement of the actuated ionomer fiber for a square-wave voltage of amplitude $\bar{\psi}=5\,\mathrm{V}$ applied to the external electrodes, for a square-wave of frequency $0.1\,\mathrm{Hz}$ (blue) and $1\,\mathrm{Hz}$ (red). Time is scaled with respect to the period T of the excitation. Data are reproduced from [8].

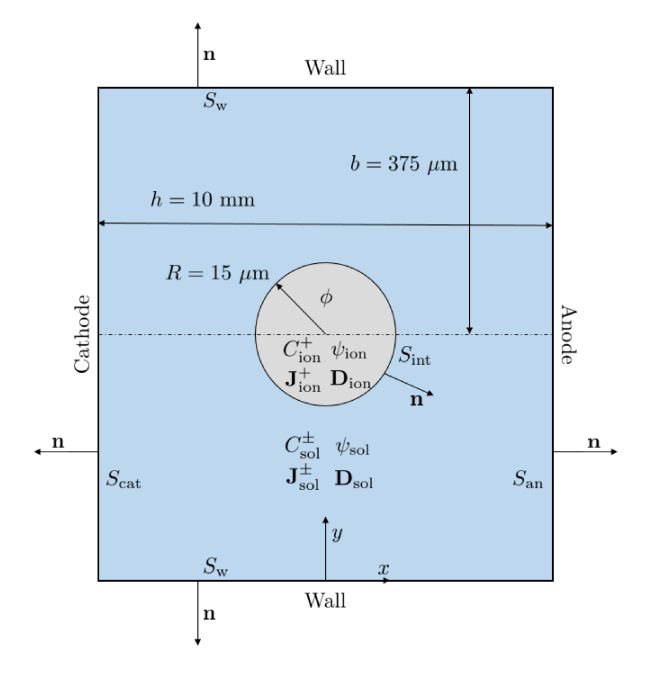


Fig. 3. Schematics of the computational domain, with the geometrical parameters of the simulation. The light blue domain indicates the solution, while the light gray domain represents the ionomer. In each domain, we show the variables defined therein. Each external and internal boundary is indicated by S_{\bullet} , where the subscript is used to differentiate parts of the boundary. Note that the schematics is not in scale, for illustration purposes.

The electrochemistry is described by the PNP system. Due to the nonlinear form of the electromigration term, closed-form analytical solutions of this system are, in general, not available for arbitrary geometries and high values of the applied voltage. For this reason, we rely on a numerical solution, which is detailed in the following section.

Mass conservation of cations and anions and the Poisson equation are expressed as [12]

$$\frac{\partial C^{\pm}}{\partial t} + \nabla \cdot \mathbf{J}_{\text{sol}}^{\pm} = 0, \tag{1a}$$

$$\nabla \cdot \mathbf{D}_{\text{sol}} = Q_{\text{sol}},\tag{1b}$$

where C^+ , C^- , $\mathbf{J}_{\text{sol}}^+$, $\mathbf{J}_{\text{sol}}^-$, \mathbf{D}_{sol} , and Q_{sol} indicate the concentrations of cations and anions per unit volume of the solution, the fluxes of cations and anions, the electric displacement, and the net charge in the solution, respectively. In addition, $\frac{\partial}{\partial t}(\cdot)$ and $\nabla(\cdot)$ represent partial derivative with respect to time and nabla operator, respectively.

We assume that the ionic fluxes are governed by the Nernst-Planck equation, modified with a steric coefficient ν that accounts for ion packing at high electric fields [14, 15]. Within this formulation, the concentration of ions in the solution cannot exceed $\frac{C_{0_{sol}}}{\nu}$, where $C_{0_{sol}}$ is the initial concentration. In addition, we suppose that the solution behaves as a dielectric material, and that there is no Faradaic reaction at the electrodes. The latter assumption is unlikely verified in [8], as the applied voltage is above the electrolysis standard potential of water. To address this issue, we focus on the highest excitation frequency of 1 Hz, for which we expect the ions in the solution to be the main current carriers. Under these hypotheses, the constitutive equations for the solution are

$$\begin{split} J_{\text{sol}}^{\pm} &= -\mathcal{D}_{\text{sol}} \left[\nabla C^{\pm} \pm \frac{\mathcal{F}C^{\pm}}{\mathcal{R}\mathcal{T}} \nabla \Psi \right. \\ &\left. + \frac{\nu C^{\pm}}{C_{0_{\text{sol}}} - \nu (C^{+} + C^{-})} \nabla (C^{+} + C^{-}) \right], \end{split} \tag{2a}$$

$$\mathbf{D}_{\text{sol}} = -\varepsilon_{\text{sol}} \nabla \psi, \tag{2b}$$

$$Q_{\text{sol}} = \mathcal{F}(C^+ - C^-). \tag{2c}$$

Here, ψ is the electric potential; \mathcal{D}_{sol} is the diffusivity of ions in solution (assumed equal for cations and anions); and \mathcal{F} , \mathcal{R} , and \mathcal{T} are the Faraday constant, the universal gas constant, and the absolute temperature, respectively.

In the ionomer, the anions are fixed, so that their concentration does not vary in time. We assume that such a concentration is also uniform and equal to $C_{0_{\text{ion}}}$. Under this hypothesis, the PNP system for the ionomer reduces to [13]

$$\frac{\partial C^{+}}{\partial t} + \nabla \cdot \mathbf{J}_{\text{ion}}^{+} = 0, \tag{3a}$$

$$\nabla \cdot \mathbf{D}_{\text{ion}} = Q_{\text{ion}}. \tag{3b}$$

Note that C^+ , in this case, is the concentration per total volume of the ionomer. Since we expect the concentration of counterions not to grow, we neglect steric effects in the ionomer. By supposing that the ionomer also behaves as a dielectric, and considering that anions are fixed, we obtain the following constitutive laws:

$$\mathbf{J}_{\text{ion}}^{+} = -\mathcal{D}_{\text{ion}} \left(\nabla C^{+} + \frac{\mathcal{F}C^{+}}{\mathcal{R}\mathcal{I}} \nabla \Psi \right), \tag{4a}$$

$$\mathbf{D}_{\text{ion}} = -\varepsilon_{\text{ion}} \nabla \psi, \tag{4b}$$

$$Q_{\text{ion}} = \mathcal{F}(C^+ - C_{0_{\text{ion}}}), \tag{4c}$$

where the diffusivity \mathcal{D}_{ion} and the dielectric constant ϵ_{ion} of the ionomer can be different from the solution.

At the anode (S_{an}) and at the cathode (S_{cat}) , we impose a time-varying voltage

$$\psi_{\text{sol}}|_{S_{\text{cat}}} = -\frac{\bar{\Psi}}{2}(t),$$
(5a)

$$\left. \psi_{\text{sol}} \right|_{S_{\text{an}}} = \frac{\bar{\Psi}}{2}(t), \tag{5b}$$

thereby neglecting the effect of the potential drop across the Stern layer [12]. On the lateral walls, instead, we require that the normal component of the electric displacement is zero, that is,

$$\mathbf{D}_{\text{sol}} \cdot \mathbf{n}|_{S_{w}} = 0. \tag{6}$$

This boundary condition implies that charges do not accumulate at the lateral walls, which is tenable for the setup of [8]. In addition, we set the ionic fluxes to zero on all the boundaries, consistent with our hypothesis of no Faradaic reactions, through the following conditions:

$$\mathbf{J}^{\pm} \cdot \mathbf{n} \big|_{S_{\text{cat}}} = \mathbf{J}^{\pm} \cdot \mathbf{n} \big|_{S_{\text{an}}} = \mathbf{J}^{\pm} \cdot \mathbf{n} \big|_{S_{\text{w}}} = 0. \tag{7}$$

To close the problem, matching conditions at the interface S between the ionomer and the solution are imposed. We require that the concentration and flux of counterions are matched per unit volume of water, whereby we rescale the values in the ionomer by its porosity ϕ , estimated from [16],

$$C_{\text{sol}}^+ \big|_{S_{\text{int}}} = \frac{C_{\text{ion}}^+}{\phi} \Big|_{S_{\text{int}}},$$
 (8a)

$$\mathbf{J}_{\mathrm{sol}}^{+} \cdot \mathbf{n} \Big|_{S_{\mathrm{int}}} = \frac{\mathbf{J}_{\mathrm{ion}}^{+}}{\phi} \cdot \mathbf{n} \Big|_{S_{\mathrm{int}}}.$$
 (8b)

As the ionomer is selectively permeable, we require that the flux of anions is zero at the interface

$$\mathbf{J}_{\mathrm{sol}}^{-} \cdot \mathbf{n} \big|_{S_{\mathrm{int}}} = 0. \tag{9}$$

Finally, we match the electric potential and the normal component of the electric displacement across the interface

$$|\Psi_{\text{sol}}|_{S_{\text{int}}} = |\Psi_{\text{ion}}|_{S_{\text{int}}},$$
 (10a)

$$\mathbf{D}_{\text{sol}} \cdot \mathbf{n}|_{S_{\text{int}}} = \mathbf{D}_{\text{ion}} \cdot \mathbf{n}|_{S_{\text{int}}}.$$
 (10b)

The latter condition ensures that no surface charge is generated at the interface.

The actuator is considered as a beam, forced by osmotic pressure and Maxwell stress that generate two internal bending moments M_{ionic} and M_{pol} , respectively, given by

$$M_{\text{ionic}} = -\mathcal{R}\mathcal{T} \int_{\Omega_{\text{ion}}} (C^+ - C_0) x \, d\Omega_{\text{ion}},$$
 (11a)

$$M_{\text{pol}} = \frac{\varepsilon_{\text{ion}}}{2} \int_{\Omega_{\text{ion}}} ||\mathbf{E}||^2 x \, d\Omega_{\text{ion}}, \tag{11b}$$

where $\mathbf{E} = -\nabla \psi$ is the electric field, $\|\cdot\|$ is the norm of a vector, and Ω_{ion} is the two-dimensional domain of the ionomer.

4 Finite element solution

We solve the electrochemical problem in the commercial finite element software COMSOL Multiphysics. We exploit symmetry with respect to the vertical plane perpendicular to the electrodes and passing through the middle of the cylinder to simulate only half of the domain (Fig. 4), toward reducing the computational cost. The presence of thin boundary layers at the electrodes and at the interface between the ionomer and the solution, in fact, requires very fine meshes, implying expensive and ill-conditioned computations. In addition, we decrease the dimension of the domain by reducing the width of the electrodes, while assuring that no interaction between the wall and the ionomer takes place.

We do not seek for quantitative agreement with experiments, as we do not have access to unknown material parameters, but we attempt at gathering qualitative information about the physics of the problem. To facilitate convergence of the simulation, we substitute the 5 V square-wave from [8] with a sinusoidal input of the same amplitude and frequency. This choice yields reduced values of the bending moments. Furthermore, we use a slightly higher value of the dielectric constant of Nafion membranes in salt solution than literature values [17], further reducing the computational cost by increasing the thickness of the boundary layers. The dielectric constant of the water is multiplied by the same factor to maintain the same ratio between the two dielectric constants. The parameters of the simulation are listed in Table 1.

At the beginning of the simulation, the steady-state solution for no external electric field applied is determined, corresponding to electrochemical equilibrium [18]. With the steady-state condition as the initial state of our system, we simulate the response over a half period to evaluate the timevarying internal bending moments in the membrane.

The time steps in the simulation are advanced through a backward differentiation formula (BDF). The standard multi-

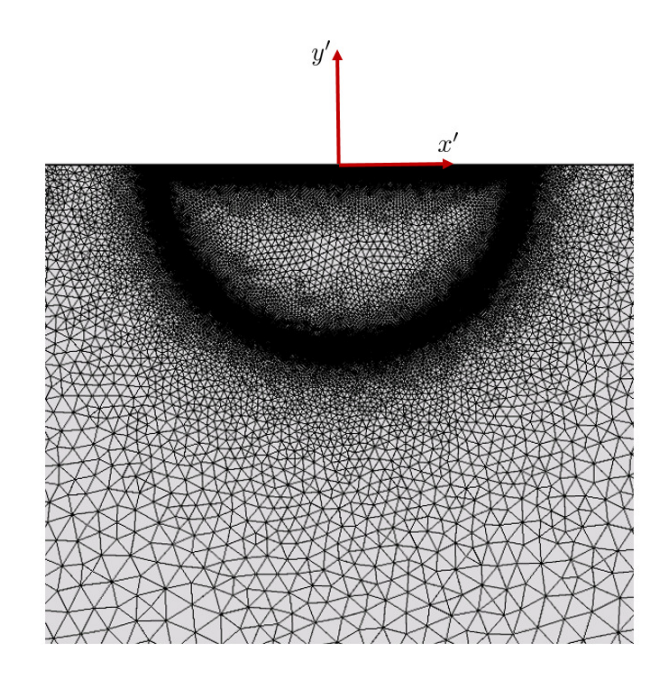


Fig. 4. Detailed view of the mesh used in the simulation, highlighting the refining of the mesh near the interface between the ionomer and the solution to properly capture boundary layers. Axes x' and y' are parallel to x and y axes in Figure 3, respectively.

| Table 1. Model parameters. | |
|---|------------------------|
| Parameter | Value |
| $\mathcal{T}[K]$ | 300 |
| $C_0 [\mathrm{mol} \; \mathrm{m}^{-3}]$ | 1070 |
| $C_{0_{\rm s}}$ [mol m ⁻³] | 100 |
| $\mathcal{D}_i \; [m^2 \; s^{-1}]$ | 3.84×10^{-10} |
| \mathcal{D}_{s} [m ² s ⁻¹] | 1×10^{-9} |
| $\epsilon_i \ [F \ m^{-1}]$ | 8.854×10^{-7} |
| $\epsilon_s \ [F \ m^{-1}]$ | 7.083×10^{-9} |
| φ | 0.3837 |

frontal massively parallel sparse direct solver (MUMPS) implemented in COMSOL is used for the solution of the sparse finite element system.

0.0033

5 Results

Figure 5 shows the simulated evolution in time of the bending moments due to ion mixing and polarization. Interestingly, we find that the contribution of Maxwell stress dominates osmotic pressure, consistent with the actuators' deflection toward the cathode. This is in line with our previous work [19], where we proposed an alternative explanation of back-relaxation in IPMCs based on Maxwell stress.

A possible explanation for the large Maxwell stress is given by the profile of the ions' concentration in the solution

at the peak response time (Fig. 6). While charges pile-up on the side facing the cathode, a considerable depletion is registered on the opposite side. This depletion of charges may be responsible for the generation of high electric fields [20], which could beget large Maxwell stresses.

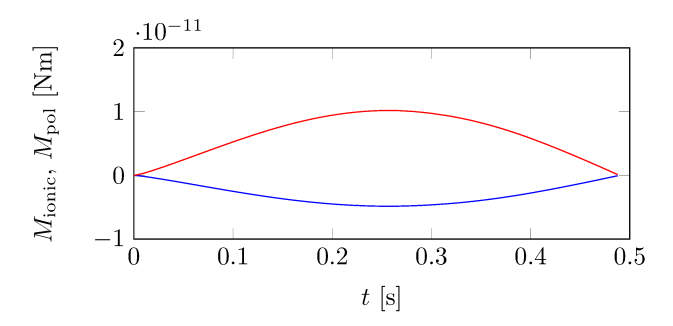


Fig. 5. Time evolution of the bending moment due to ion mixing (blue) and polarization (red) over a half period for a sinusoidal input voltage $\bar{\Psi}(t)$ with amplitude of $5\,\mathrm{V}$ and frequency of $1\,\mathrm{Hz}$.

For the time at which the voltage reaches its peak value, we examine the distribution of the electric field (Fig. 7). First, we note that the electric field near the interface is much larger than the electric field in the bulk of the solution. Second, the electric field primarily develops along the radial direction. Third, consistent with the sign of the bending moment related to the polarization (Fig. 5), the electric field is slightly higher on the side of the ionomer facing the anode, thereby causing the Maxwell stress to elicit bending moment toward the cathode. This difference should be traced back to the charge imbalance (Fig. 6), which is dissimilar on the two sides of the ionomer cilia. The ultimate explanation of this behavior is the selective permeability of the ionomer, which allows charge pile-up and depletion on the two sides, limited by two-dimensional transport phenomena.

To better support our third claim above and shed further light on the physics of actuation, in Fig. 8 we compare the nondimensional magnitude of the electric field on the surface of the cilia at the initial time and at the time at which we register the peak voltage. While showing a clear trend, the data display high frequency noise, likely related to numerical issues in the evaluation of the gradient of the potential near the interface. (Three factors may contribute to this issue: the high density of the mesh near the interface, the error in defining the curved surface of the cilia in the by mesh triangulation, and the presence of steep boundary layers.) At the initial time, we find a non-zero electric field, due to counterions' migration and formation of a Donnan potential in the bulk of the ionomer, which is lower than the potential in the solution [18]. However, the value of the electric field is uniform over all the surface, thereby causing a zero bending moment. At the time in which the voltage reaches its peak value, instead, the distribution of the electric field is skew-symmetric. Consistent with our claims in regards to Fig. 7, we observe a decrease in the norm of the electric field on the side of the ionomer facing the cathode (0 to $\frac{\pi}{2}$), and an increase on the anode side ($\frac{\pi}{2}$ to π). This symmetry break elicits the net bending moment that is the main driving phenomenon of the ionomer motion.

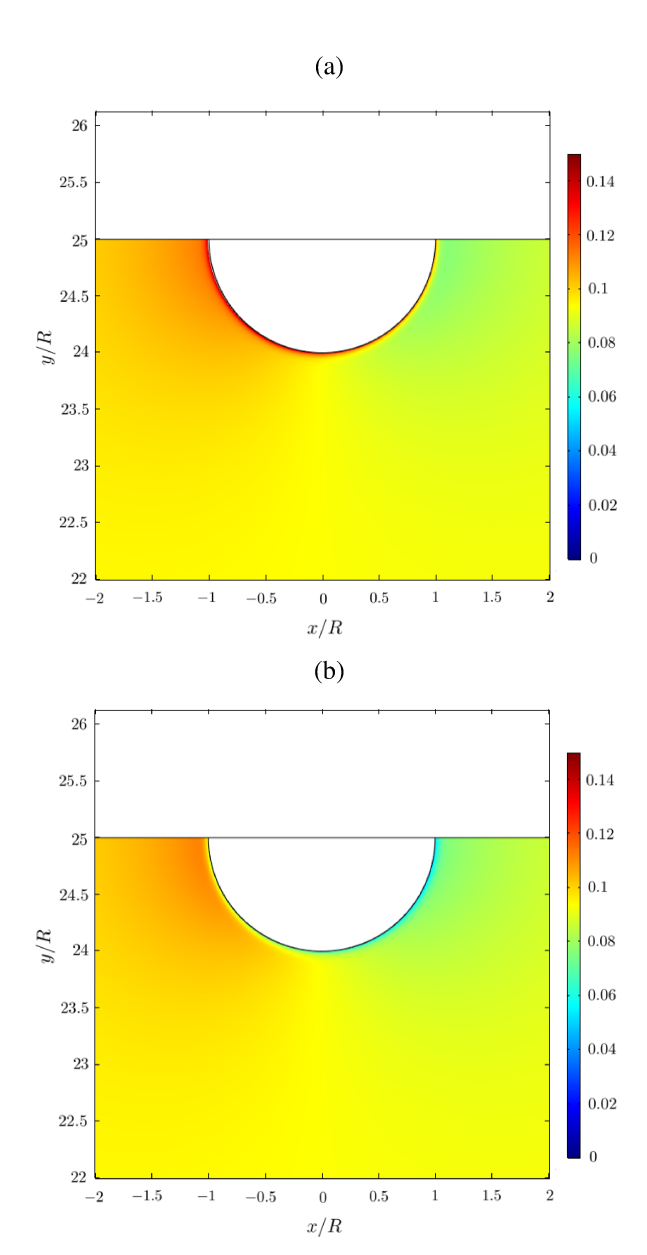


Fig. 6. Colormaps of the concentrations of cations (a) and anions (b) in the solution for $t=0.25\,\mathrm{s}$. The scale on the right indicates the ratio between the actual concentration and the concentration of the anions in the ionomer.

6 Conclusion

Here, we have proposed a model to study the actuation of ionomer fibers immersed in salt solution and subjected to an external electric field. In this model, electrochemistry, decoupled from the deformation, is solved through finite element analysis, from which the internal bending moments due to ion mixing and polarization are computed. We find that the contribution related to Maxwell stress prevails over osmotic pressure. The results of this work can inform the design of ionomer cilia-like actuators for biomimetic applications.

Acknowledgements

This research was supported by the National Science Foundation under Grant No. OISE-1545857 and by KIST flagship program under Project No. 2E29460.

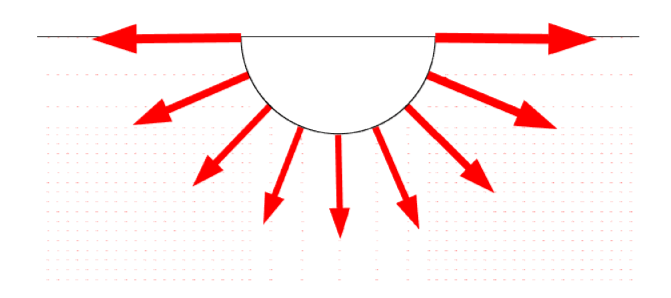


Fig. 7. Arrow surface representing the gradient of the electric potential $(-\mathbf{E})$ in the vicinity of the ionomer cilia for t=0.25 s.

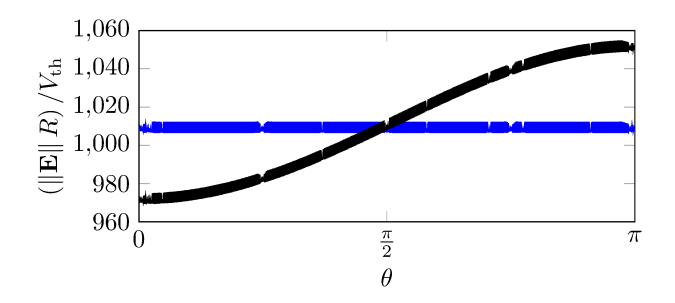


Fig. 8. Nondimensional electric field over the surface of the ionomer at the initial time (blue) and at t=0.25 s (black). θ indicates the angle between the point on the surface and the normal to the cathode, taken as 0 at the nearest point to the cathode. The electric field is nondimensionalized with $\frac{V_{\rm th}}{R}$, where $V_{\rm th}=\frac{\Re \mathcal{T}}{\mathcal{F}}$ is the thermal voltage and R is the radius of the cilia.

References

- [1] Carrico, J. D., Tyler, T., and Leang, K. K., 2017. "A comprehensive review of select smart polymeric and gel actuators for soft mechatronics and robotics applications: fundamentals, freeform fabrication, and motion control". *International Journal of Smart and Nano Materials*, **8**(4), pp. 144–213.
- [2] Stalbaum, T., Trabia, S., Hwang, T., Olsen, Z., Nelson, S., Shen, Q., Lee, D.-C., Kim, K. J., Carrico, J., Leang, K. K., Palmre, V., Nam, J., Park, I., Tiwari, R., Kim, D., and Kim, S., 2018. "Guidelines for making ionic polymer-metal composite (IPMC) materials as artificial muscles by advanced manufacturing methods". In Advances in Manufacturing and Processing of Materials and Structures, Y. Bar-Cohen, ed. CRC Press, ch. 15.
- [3] Bhandari, B., Lee, G.-Y., and Ahn, S.-H., 2012. "A review on IPMC material as actuators and sensors: Fabrications, characteristics and applications". *International Journal of Precision Engineering and Manufacturing*, **13**(1), pp. 141–163.
- [4] Jo, C., Pugal, D., Oh, I.-K., Kim, K. J., and Asaka, K., 2013. "Recent advances in ionic polymer—metal composite actuators and their modeling and applications". *Progress in Polymer Science*, 38(7), pp. 1037–1066.
- [5] Shahinpoor, M., ed., 2015. *Ionic Polymer Metal Composites (IPMCs): Smart Multi-Functional Materials and Artificial Muscles*. Smart Materials Series. Royal Society of Chemistry.

- [6] Chen, Z., 2017. "A review on robotic fish enabled by ionic polymer—metal composite artificial muscles". *Robotics and Biomimetics*, **4**(24).
- [7] Cha, Y., and Porfiri, M., 2014. "Mechanics and electrochemistry of ionic polymer metal composites". *Journal of the Mechanics and Physics of Solids*, **71**, pp. 156–178
- [8] Kim, K. J., Palmre, V., Stalbaum, T., Hwang, T., Shen, Q., and Trabia, S., 2016. "Promising developments in marine applications with artificial muscles: Electrodeless artificial cilia microfibers". *Marine Technology Society*, 50(5), pp. 24–34.
- [9] Boldini, A., Rosen, M., Cha, Y., and Porfiri, M., 2019. "Contactless actuation of perfluorinated ionomer membranes in salt solution: an experimental investigation". *Scientific Reports*, **9**(1), pp. 1–14.
- [10] Porfiri, M., Sharghi, H., and Zhang, P., 2018. "Modeling back-relaxation in ionic polymer metal composites: The role of steric effects and composite layers". *Journal of Applied Physics*, **123**(014901).
- [11] Bard, A. J., and Faulkner, L. R., 2001. *Electrochemical Methods Fundamentals and Applications*. John Wiley & Sons.
- [12] Bazant, M. Z., Thornton, K., and Ajdari, A., 2004. "Diffuse-charge dynamics in electrochemical systems". *Physical Review E*, **70**(021506).
- [13] Porfiri, M., 2008. "Charge dynamics in ionic polymer metal composites". *Journal of Applied Physics*, **104**(10).
- [14] Kilic, M. S., Bazant, M. Z., and Ajdari, A., 2007. "Steric effects in the dynamics of electrolytes at large applied voltages. I. Double-layer charging". *Physical Review E*, **75**(2).
- [15] Kilic, M. S., Bazant, M. Z., and Ajdari, A., 2007. "Steric effects in the dynamics of electrolytes at large applied voltages. II. Modified Poisson-Nernst-Planck equations". *Physical Review E*, **75**(2).
- [16] Nemat-Nasser, S., and Li, J. Y., 2000. "Electromechanical response of ionic polymer-metal composites". *Journal of Applied Physics*, **87**(7).
- [17] Mauritz, K. A., and Fu, R.-M., 1988. "Dielectric relaxation studies of ion motions in electrolyte-containing perfluorosulfonate ionomers. 1. NaOH and NaCl systems". *Macromolecules*, **21**, pp. 1324–1333.
- [18] Moya, A. A., 2015. "Theory of the formation of the electric double layer at the ion exchange membrane-solution interface". *Physical Chemistry Chemical Physics*, **17**, pp. 5207–5218.
- [19] Porfiri, M., Leronni, A., and Bardella, L., 2017. "An alternative explanation of back-relaxation in ionic polymer metal composites". *Extreme Mechanics Letters*, **13**, pp. 78–83.
- [20] Chu, K. T., and Bazant, M. Z., 2005. "Electrochemical thin films at and above the classical limiting current". *SIAM Journal of Applied Mathematics*, **65**(5), pp. 1485–1505.